

120 Gbit/s 2×2 Vector-Modes-Division-Multiplexing DD-OFDM-32QAM Free-Space Transmission

Volume 8, Number 6, December 2016

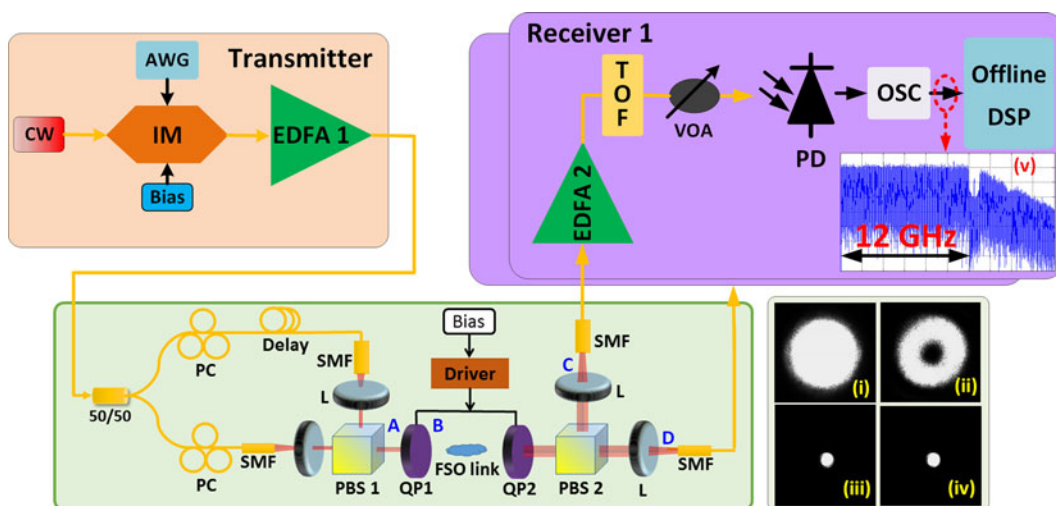
Jianbo Zhang

Fan Li

Jianping Li, Member, IEEE

Yuanhua Feng

Zhaohui Li



DOI: 10.1109/JPHOT.2016.2622859

1943-0655 © 2016 IEEE

120 Gbit/s 2 × 2 Vector-Modes-Division-Multiplexing DD-OFDM-32QAM Free-Space Transmission

Jianbo Zhang,¹ Fan Li,² Jianping Li,¹ Member, IEEE,
Yuanhua Feng,^{1,2} and Zhaohui Li^{1,2}

¹Guangdong Provincial Key Laboratory of Optical Fiber Sensing and Communications,
Institute of Photonics Technology, Jinan University, Guangzhou 510630, China

²State Key Laboratory of Optoelectronic Materials and Technologies, School of Electronics
and Information Technology, Sun Yat-sen University, Guangzhou 510275, China

DOI: 10.1109/JPHOT.2016.2622859

1943-0655 © 2016 IEEE. Translations and content mining are permitted for academic research only.
Personal use is also permitted, but republication/redistribution requires IEEE permission.
See http://www.ieee.org/publications_standards/publications/rights/index.html for more information.

Manuscript received September 23, 2016; revised October 24, 2016; accepted October 25, 2016.
Date of publication October 28, 2016; date of current version November 28, 2016. This work was
supported in part by The National High Technology 863 Research and Development of China under
Grant 2015AA017102; in part by the National Science Foundation of China under Grant 61575082,
Grant 61601199, Grant 61525502, Grant 61435006, and Grant 61490715; in part by the Guangdong
Provincial Natural Science Foundation under Grant 2015A030313328, and in part by the Fundamental
Research Funds for the Central Universities under Grant 21615450. Corresponding author: Jianping Li
(e-mail: jpli@live.cn).

Abstract: We demonstrate a 120-Gbit/s mode-division-multiplexing (MDM) system based on two typical vector modes of TE01 and TM01 with direct detection orthogonal frequency division multiplexing (DD-OFDM) and 32-quadrature-amplitude-modulation (32-QAM) signal. The vector mode conversion is achieved by the key q-plate and the mode crosstalk between the converted two vector modes are both less than -20 dB. This crosstalk can be further minimized by high-quality q-plate. In this demonstration, error-free transmission has been realized with the power penalties less than 2 dB. The experimental results show that the scheme proposed in this paper can be a good candidate in large-capacity short-reach optical interconnect.

Index Terms: Vector mode, mode-division-multiplexing (MDM), direct detection orthogonal frequency division multiplexing (DD-OFDM), optical interconnect.

1. Introduction

With the rapid increase of the data traffic, such as online videos, games, and business, the capacity of optical transmission system is urgently desired to be improved in the field of optical communication. In the long-haul transmission system, vector optical signal transmission coherent detection with digital signal processing (DSP) technique in the transceiver side has been successfully applied to realize large capacity signal transmission [1]. Additionally, the few-mode fiber (FMF) based mode-division-multiplexing (MDM) and multicore fiber (MCF) based spatial division multiplexing (SDM) have been gained a lot of research attention recently [2]–[4]. In general, the fiber modes used in FMF-MDM systems are linearly-polarized modes (LPM) as the individual channels and transmission capacity can be significantly increased by incorporating with FM multi-core fiber (FM-MCF) [5]. While in the short reach, it is still difficult to realize 100 Gbit/s and beyond bit rate signal transmission. Optical interconnect is proposed to be a solution for up to 400 Gbit/s signal transmission in the short reach [6], but in the short reach optical interconnect, the coherent detection

technique has been abandoned due to its high power consumption and cost. Intensity modulation and direct detection (IM/DD) gradually shows its potential in constructing low cost and low power consumption optical interconnect systems. Thus, the IM/DD based technologies regarding capacity enhancement and cost and power consumption control become a hot spot in optical interconnect in nowadays [6]–[8].

To improve the capacity of the short reach optical interconnect, the MDM based technology has also been exploited, including the LP modes, OAM modes and vector modes [9]–[14]. However, most of these demonstrations are based on the coherent detection even for the propagating in free space optical link. For instance, the VM-based MDM coherent (VMDM-CO) transmission over FSO link has been demonstrated in [14]. In this experiment, four degenerated VMs consisted of the LP11 mode group of a fiber supported, i.e., the TE01, TM01, HE21^{odd} and HE21^{even}, have been exploited to the VMDM channels. While these demonstrations may be not appropriate for optical interconnect due to high cost and the intricacy of the structure.

In principle, direct detection scheme can be combined with LPM-based or VM-based MDM technology to increase the capacity of optical transmission systems. Furthermore, MDM transmission can be realized without sophisticated DSP [15]–[16]. Meanwhile, orthogonal frequency division multiplexing (OFDM) technology, which has high transmit speed with high spectrum efficiency, has been adopted widely in the field of optical communication in virtue of its capability of overcoming multipath fading and inter symbol interference (ISI) on frequency selective channels in a very effective way [17]–[21]. DD-OFDM is also a competitive candidate in the realization of optical interconnect, while OFDM signal in these systems are only transmitted over fundamental mode, the bandwidth requirement of optical and electrical devices should be very high when beyond 100 Gbit/s signal is transmitted over fundamental mode, the cost of the whole system will be very expensive [17]–[21]. DD-OFDM with VMDM can be used to reduce the cost of system while still maintaining the total bit rate larger than 100 Gbit/s. When several VMs used to transmit signal simultaneously, the bandwidth of signal on each VM can be significantly reduced, and thus, the cost can be easily controlled.

In this paper, unlike the previous works with the coherent detection in VMDM system, we demonstrate the VMDM based DD-OFDM transmission with higher-order modulation formats for optical interconnect. By using the basic two VMs, TE01 and TM01, and 32QAM modulation format OFDM signal, we have successfully realized a 120 Gbit/s transmission over ~80 cm FSO link without multiple-input multiple-output (MIMO) DSP processing in the lab. On the one hand, our proposal satisfies the demand for favorable performance and large capability systems by using VM-based MDM. on the other hand, the method of direct detection is cost-effective and has more simple structure. The results show that the VMs of fiber could have the potential in the MDM-DD-OFDM transmission in short-reach optical interconnect.

2. Test Results of Used Q-Plates

For the demonstrated VMDM-DD-OFDM system, the q-plates (QPs) also called variable spiral plate (VSP), are the key components of mode conversion. QP is a passive liquid crystal optical element that has the ability to modify the spatial distribution of the polarization of a homogenous polarized beam and has been studied widely [22]–[25]. Thus, q-plate is one kind of mode converter which is similar to the phase-plate for LP modes and spatial light modulator for OAM modes. With q-plate, whose optical axis orientation α in the xy plane can be expressed as [26]

$$\alpha(r, \varphi) = q\varphi + \alpha_0 \quad (1)$$

where r and φ represent the points on the transverse plane in polar coordinates, q is the topological charge, and α_0 is a constant offset angle. The q-plate in our lab is the one produced by Arcoptix with $q = 1/2$ [27]. It is flexible and convenient to introduce Jones matrix to analyze the function of QP in our experiment. The Jones matrix of QP can be described as \mathbf{J}_s [26]

$$\mathbf{J}_s = \begin{pmatrix} \cos 2\alpha & \sin 2\alpha \\ \sin 2\alpha & -\cos 2\alpha \end{pmatrix} \quad (2)$$

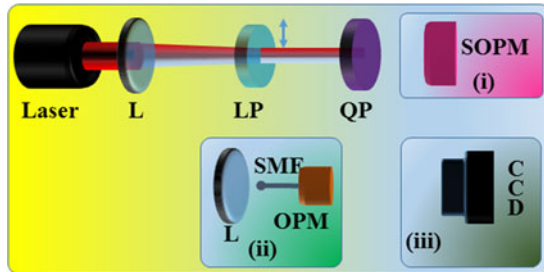


Fig. 1. Experimental setup for q-plate characterization by using (i) spatial optical power meter (SOPM), (ii) common OPM, and (iii) charged-coupled device (CCD) camera. L: lens; LP: linear polarizer.

In this equation, α represents the optical axis orientation in the transverse plane according to (1). The light field of linear polarized beam can also be described with a Jones vector \mathbf{E}_{in} , such as horizontal and vertical polarizations given by $(1 \ 0)^T$ and $(0 \ 1)^T$. After passing through the QP, the output light \mathbf{E}_{out} can be expressed as follows:

$$\mathbf{E}_{\text{out}} = \mathbf{J}_s \mathbf{E}_{\text{in}} \quad (3)$$

Theoretically, VMs are the solutions of wave equation in cylindrical coordinates. The polarization state of VMs can be given by the Jones vector [28]

$$|\ell, \gamma\rangle = (\cos(\ell\varphi + \gamma) \sin(\ell\varphi + \gamma))^T \quad (4)$$

where $\ell = \pm 1, \pm 2, \dots$, and $\gamma = 0, \pi/2$. Jones vector $(\cos\varphi \sin\varphi)^T$ and $(-\sin\varphi \cos\varphi)^T$ correspond to radial and azimuthal polarization beams, respectively. For instance, $V_{+1,0}$ and $V_{+1,\pi/2}$ are radial (TM01 mode) and azimuthal (TE01 mode) polarization, respectively. The conversion from homogeneous linear polarized beam to such as radial, azimuthal can simply be obtained by placing the q-plate in the optical path of the laser beam. Then by simply changing the bias voltage applied on the q-plate, the different output polarization patterns can be obtained. The experimental setup of the characterization of the used q-plates is shown in Fig. 1.

We first show the output power vs. the applied bias voltage V_b , which can help us to choose appropriate bias to the subsequent data transmission. The input cw laser source with its center wavelength of 1549.994 nm and power of 12.5 dBm, is first collimated by the lens (L) and then fed into the QP via linear polarizer (LP), after the conversion to the VM, the received power has been detected by (i) the spatial optical power meter (SOPM) and (ii) common power meter with pigtailed single mode fiber (OPM), respectively. Meanwhile, the intensities of generated VMs are captured by (iii) the charge-coupled device (CCD) camera.

The measured property of optical power vs. applied voltage V_b of the two QPs are shown in Fig. 2(a) and Fig. 2(b) respectively corresponding to the cases of (i) and (ii) in Fig. 1. We can see that the whole received optical power of the two QPs always keeps the same level within the range of V_b from 0 to 4.2 V, except for $\sim 11\%$ lower within the range [0 1.2] V. The insertion loss of each QP is about ~ 5 dB which is higher than that in [17] at the laser's wavelength. However, the received optical power by using OPM keep relatively stable within the range of V_b from 0 to 1.2 V, whereas it goes up rapidly when $V_b > 1.2$ V. This result shows that the used QPs in our lab can convert the fundamental mode to vector modes efficiently when $V_b \leq 1.2$ V at the laser's wavelength. If $V_b > 1.2$ V, there are more power of input laser that cannot be converted to the VMs with the increasing V_b . However, the properties of the two QPs can be treated the same even with slight difference. The insets show the corresponding intensity profiles when V_b is equal to 0.1, 2.0 and 4.2 V, respectively. Obviously, the higher-order VM with doughnut-like intensity has been achieved under the regular operation region (ROR), and no VM can be obtained under the non-operational region (NOR). Between the ROR and NOR, there are few VMs mixed fundamental mode can be found if the V_b is applied in the partial operational region (POR).

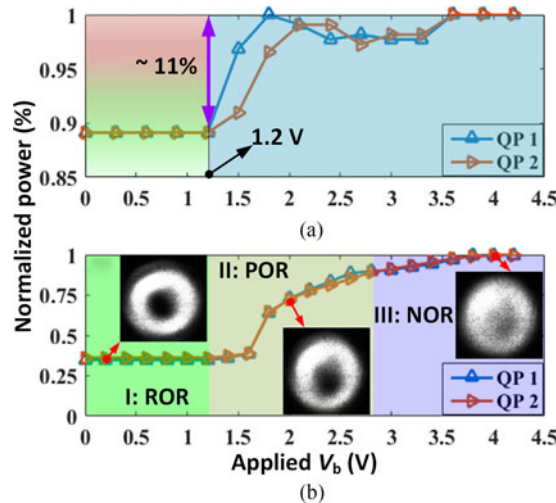


Fig. 2. The normalized power vs. applied V_b based on (a) SOPM and (b) OPM. ROR: regular operational region; POR: partial operational region; NOR: non-operational region; V_b : bias voltages.

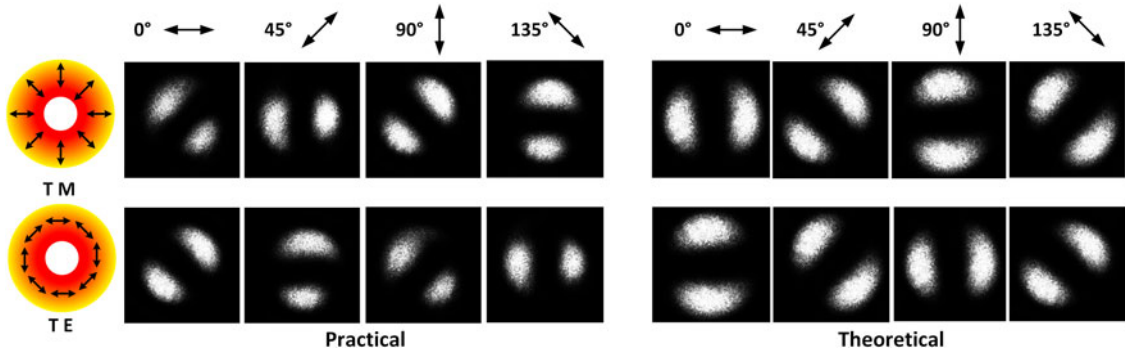


Fig. 3. Property of converted VMs characterized by LP and CCD, where the arrows indicate the orientations of the transmission axis of the LP.

3. Experiment, Results, and Discussion

Then we do the characterization of VM conversion property of the two QPs. At this time, by rotating the LP placed in front of the CCD camera to a specific angle, intensity profiles can be shown and then used to identify the property of converted VMs. According to the above analysis, we set the V_b to 0 V. The experimental results are shown in Fig. 3. We can see that the TE01 (azimuthal polarization) and TM01 (radial polarization) VMs can be generated effectively except there is $\sim 45^\circ$ rotation of the direction. This rotation is mainly induced by the constant offset angle α_0 of QPs while it has no influence on the transmission performance. The VM's crosstalk has been shown in Fig. 4, in which a mode isolation (MI) larger than 20 dB can be obtained when the two orthogonal VMs are transmitted. This MI can be used to implement the direct-detected optical transmission without MIMO DSP and then result in the potential in short-reach optical interconnect. Therefore, this is our study goal to demonstrate the feasibility of high-speed data transmission based on VMDM-DD with OFDM modulation.

Fig. 5 shows the experimental setup for the VMDM-DD-OFDM transmission system. At the optical transmitter, there is an external cavity laser (ECL) at 1549.994 nm with less than 100-kHz linewidth and maximum output power of 14.5 dBm. The continuous-wavelength (CW) lightwave from ECL is modulated by intensity modulator (IM, Photoline MX-LN-40) driven by an electrical baseband OFDM

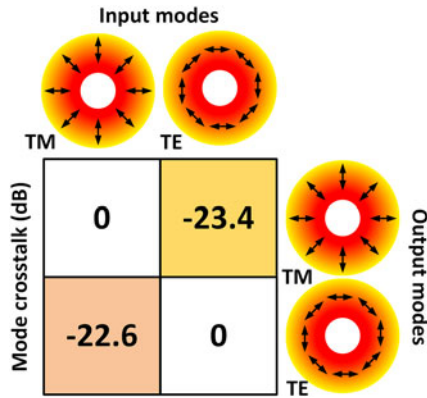


Fig. 4. Mode crosstalk of used q-plates.

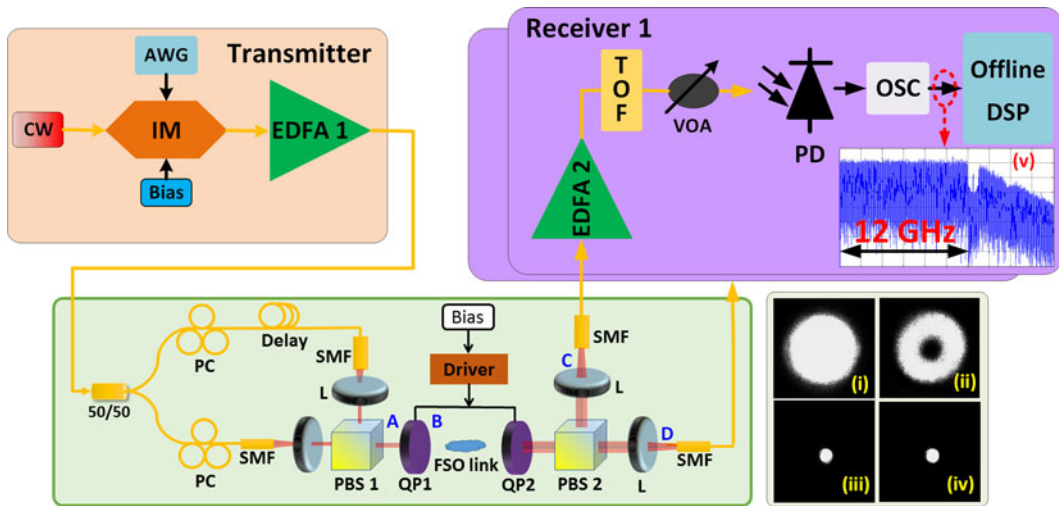


Fig. 5. Experimental setup for DD-OFDM-VMMMD based optical transmission. CW: continuous wave; IM: intensity modulator; AWG: arbitrary waveform generator; EDFA: Erbium-doped fiber amplifier; PC: polarization controller; SMF: single mode fiber; L: lens; PBS: polarization beam splitter; QP: q-plate; VOA: variable optical attenuator; PD: photo-detector; OSC: oscilloscope.

signal. The OFDM signal is generated by an arbitrary waveform generator (AWG, Tektronix AWG 70002A) with a 25 Gs/s sampling rate, and its V_{pp} is 1 V. Here, the fast Fourier Transform (FFT) size for OFDM generation is 512 and the subcarrier symbol rate is 48.83 MS/s, in which 492 subcarriers are employed with 246 conveying data in the positive frequency bins, the first subcarrier is set to zero for DC-bias and the rest 19 null subcarriers at the edge are reserved for oversampling. Symbols with 32-QAM modulation format will be loaded on all the 246 information-bearing subcarriers. A 32-sample cyclic prefix is added to the 512 samples, giving 544 samples per OFDM symbol. One training symbol (TS) is inserted before every 100 OFDM data symbols to realize time synchronization and channel response acquisition. The baseband OFDM signal generated by above mentioned AWG is first boosted by one linear electrical amplifier and then injected into IM. For optical OFDM modulation, the half-wave voltage of the MZM in this experiment is 3.4 V, and MZM is biased at 1.9 V at its linear region. As far as we know, the maximum power limit of Q-plate is about 26 dBm. Then, the generated optical OFDM signal is injected into an EDFA (EDFA1, the saturated output power is \sim 20 dBm) to control the launch power into VM conversion and multiplexing parts. Thus, the power level at the optical transmitter is below the safe power level for our free-space communication system.

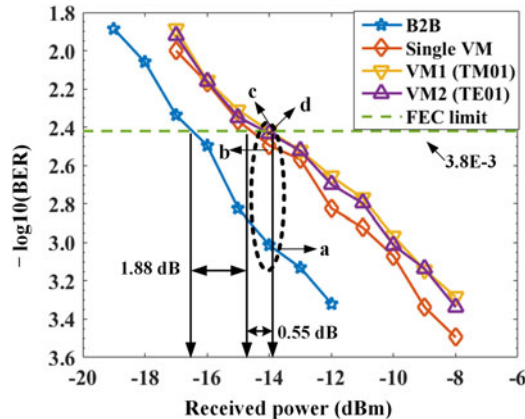


Fig. 6. BER performance vs. received power of the VMDM-DD-OFDM transmission. B2B: back-to-back.

After FSO transmission, the optical OFDM signal is mode re-converted by the QP2 and then de-multiplexed by the PBS. Insets (i) ~ (iv) show the intensity profiles corresponding to the linear combination of horizontal and vertical polarization of the fundamental mode (A point), multiplexed VMs (B point), and the two de-multiplexed VM channels (C and D points); then, the optical OFDM signal is pre-amplified by another EDFA (EDFA2, output power is ~ 16 dBm) and then filtered by a 1-nm bandwidth tunable optical filter (TOF) to block the out-band ASE noise. A variable optical attenuator (VOA) is applied to adjust the received optical power for sensitivity measurement and then optical-to-electrical (O/E) conversion is implemented via an optical receiver (u2t XPDV2120R) with 3-dB bandwidth of 50 GHz. The converted electrical signal was sampled by a real-time oscilloscope (OSC, LecroyLabMaster 10-36Zi) and processed off-line with a sampling rate of 40 GSa/s. The resolution of the DAC in AWG and ADC in real-time OSC used at the transmitter and receiver are both 8-bit. Insets (v) shows the electrical spectrum of the received signal. The captured signal is then further processed in the laptop for the off-line digital signal processing (DSP). The off-line DSP procedure contains CP removal, FFT, channel estimation with Intra-symbol frequency-domain averaging (ISFA) [29], one-tap equalization, and 32-QAM de-mapping and bit-error ratio (BER) calculation. In the calibration stage, pre-equalization is realized to overcome high frequency power attenuation induced serious intra-symbol interference (ISI) [30]. In this letter, one OFDM symbol contains 1230 bits and the BER was obtained by direct error counting with 500 OFDM symbols ($1230 \times 500 = 615\,000$ bits). The raw bit rate on each vector mode in the system is 60.06 Gb/s ($25 \times 246/512 \times 5$ Gb/s ≈ 60.06 Gb/s), the total raw bit rate is 120.12 Gbit/s with two modes are used to transmit OFDM signal. After excluding all the overheads including TS, CP and 7% hard decision forward-error-correction (HD-FEC) we can realize 104.61 Gb/s net bit rate signal transmission.

Fig. 6 shows the measured BER property versus the received optical power. We can see that there is a 1.88 dB power penalty between the single VM channel and “back to back” (B2B) transmission where the optical OFDM signal is directly sent to PD without propagating through 80-cm FSO. When the two VMs are transmitted simultaneously, only 0.55 dB power penalty is induced. This shows that the error-free transmission of 120 G VMDM-DD-OFDM can be achieved easily. Fig. 7 shows the constellations of the demodulated OFDM/32QAM signals corresponding to the cases of B2B, single VM, and two VM channels (dotted-circle in Fig. 6) when received power equals -14 dBm. This further shows the little difference of performance with a comparison of single VM and VM multiplexed transmissions.

4. Conclusion

In conclusion, we have demonstrated the vector-mode-division-multiplexing based direct-detection OFDM transmission over free space optical link. The higher order vector modes are converted based on the q-plate, which has been gained so much interest in various kinds of studies recently.

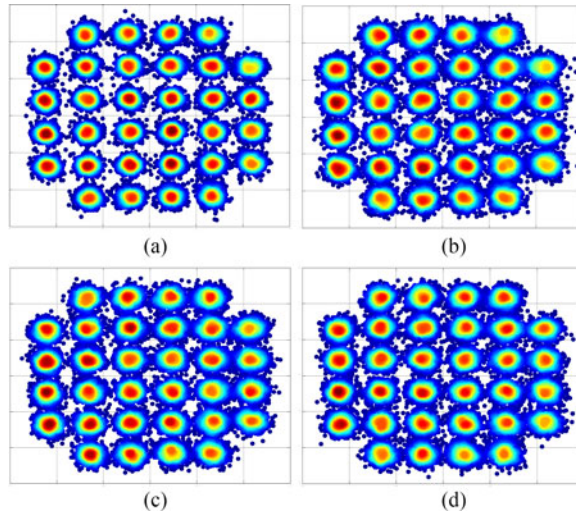


Fig. 7. Constellations for the four cases correspond to the dotted-circle in Fig. 6 when the received optical power is -14 dBm.

The performance of the used q-plates has been characterized to implement the VMDM-DD-OFDM transmission with proper operation conditions to avoid the MIMO processing. A 120Gb/s 2×2 VMDM-DD-OFDM signal has been successfully transmitted over ~ 80 cm FSO link without MIMO DSP processing. If the key component—q-plates in our experiment—have higher efficiency of mode conversion, the system performance of demonstrated can be improved significantly. To our best knowledge, this is the first demonstration of the vector modes (azimuthal and radial polarization modes) based MDM-DD-OFDM transmission with data rate over 100 Gbit/s. The experimental results show that VMDM-based DD-OFDM transmission would be a good candidate in short-reach optical interconnect systems.

References

- [1] S. Savory, "Digital coherent optical receivers: Algorithms and subsystems," *IEEE J. Sel. Topics Quantum Electron.*, vol. 16, no. 5, pp. 1164–1179, Sep./Oct. 2010.
- [2] G. M. Saridis, D. Alexandropoulos, G. Zervas, and D. Simeonidou, "Survey and evaluation of space division multiplexing: From technologies to optical networks," *IEEE Commun. Surv. Tuts.*, vol. 17, no. 4, pp. 2136–2156, Oct.–Dec. 2015.
- [3] G. Li, N. Bai, N. Zhao, and C. Xia, "Space-division multiplexing: The next frontier in optical communication," *Adv. Opt. Photon.*, vol. 6, pp. 413–487, 2014.
- [4] P. Winzer, "Making spatial multiplexing a reality," *Nat. Photon.*, vol. 8, 2014, Art. no. 345.
- [5] R. Uden *et al.*, "Ultra-high-density spatial division multiplexing with a few-mode multicore fibre," *Nat. Photon.*, vol. 8, 2014, Art. no. 865.
- [6] IEEE, P802.3bs 400 Gb/s Ethernet Task Force. (2015). [Online]. Available: <http://www.ieee802.org/3/bm/index.html>
- [7] F. Karinou, R. Borkowski, D. Zibar, and I. Roudas, "Advanced modulation techniques for high performance computing optical interconnects," *IEEE J. Sel. Topics Quantum Electron.*, vol. 19, no. 2, Mar./Apr. 2013, Art. ID 3700614.
- [8] X. Xu *et al.*, "Advanced modulation formats for 400-Gbps short-reach optical inter-connection," *Opt. Exp.*, vol. 23, no. 1, pp. 492–500, 2015.
- [9] H. Wen *et al.*, "First demonstration of 6-mode PON achieving a record gain of 4 dB in upstream transmission loss budget," *J. Lightw. Technol.*, vol. 34, no. 8, pp. 1990–1996, Apr. 2016.
- [10] J. Wang *et al.*, "Terabit free-space data transmission employing orbital angular momentum multiplexing," *Nat. Photon.*, vol. 6, pp. 488–496, 2012.
- [11] A. Willner *et al.*, "Optical communications using orbital angular momentum beams," *Adv. Opt. Photon.*, vol. 7, no. 1, pp. 66–106, 2015.
- [12] T. Lei *et al.*, "Massive individual orbital angular momentum channels for multiplexing enabled by dammann gratings," *Light, Sci. Appl.*, vol. 4, 2015, Art. no. e257.
- [13] N. Bozinovic *et al.*, "Terabit-scale orbital angular momentum mode division multiplexing in fibers," *Science*, vol. 340, no. 6140, pp. 1545–1548, 2013.
- [14] G. Milione *et al.*, "4x20Gbit/s mode division multiplexing over free space using vector modes and a q-plate mode (de)multiplexer," *Opt. Lett.*, vol. 40, no. 9, pp. 1980–1983, 2015.

- [15] E. Ip *et al.*, "SDM transmission of real-time 10GbE traffic using commercial SFP + transceivers over 0.5km elliptical-core few-mode fiber," *Opt. Exp.*, vol. 23, no. 13, pp. 17120–17126, 2015.
- [16] J. Luo, J. Li, Q. Sui, Z. Li, and C. Lu, "40Gb/s Mode-division multiplexed DD-OFDM transmission over standard multi-mode fiber," *IEEE Photon. J.*, vol. 8, no. 3, Jun. 2016, Art. ID 790527.
- [17] Z. Cao, J. Yu, W. Wang, L. Chen, and Z. Dong, "Direct-detection optical OFDM transmission system without frequency guard band," *IEEE Photon. Technol. Lett.*, vol. 22, no. 11, pp. 736–738, Jun. 2010.
- [18] Z. Cao *et al.*, "A synchronized signaling insertion and detection scheme for reconfigurable optical OFDM access networks," *J. Lightw. Technol.*, vol. 30, no. 24, pp. 3972–3979, Dec. 2012.
- [19] J. Yu, M.-F. Huang, D. Qian, L. Chen, and G.-K. Chang, "Centralized lightwave WDM-PON employing 16-QAM intensity modulated OFDM downstream and OOK modulated upstream signals," *IEEE Photon. Technol. Lett.*, vol. 20, no. 18, pp. 1545–1548, Sep. 2008.
- [20] M. Chen *et al.*, "Improved BER performance of real-time DDO-OFDM systems using interleaved Reed–Solomon codes," *IEEE Photon. Technol. Lett.*, vol. 28, no. 9, pp. 1014–1017, May 2016.
- [21] M. Chen, J. He, Q. Fan, Z. Dong, and L. Chen, "Experimental demonstration of real-time high-level QAM-encoded direct-detection optical OFDM systems," *J. Lightw. Technol.*, vol. 33, no. 22, pp. 4632–4639, Nov. 2015.
- [22] P. Gregg *et al.*, "Q-plates as higher order polarization controllers for orbital angular momentum modes of fiber," *Opt. Lett.*, vol. 40, no. 8, 1729–1732, 2015.
- [23] Y. S. Rumala *et al.*, "Tunable supercontinuum light vector vortex beam generator using a q-plate," *Opt. Lett.*, vol. 38, no. 23, pp. 5083–5086, 2013.
- [24] L. Yan *et al.*, "Q-plate enabled spectrally diverse orbital-angular-momentum conversion for stimulated emission depletion microscopy," *Optica*, vol. 2, no. 10, pp. 900–903, 2015.
- [25] D. Naidoo *et al.*, "Controlled generation of higher-order Poincaré sphere beams from a laser," *Nat. Photon.*, vol. 10, pp. 327–332, 2016.
- [26] L. Marrucci, C. Manzo, and D. Paparo, "Optical spin-to-orbital angular momentum conversion in inhomogeneous anisotropic media," *Phys. Rev. Lett.*, vol. 96, no. 16, p. 163905, 2006, Art. no. 163905.
- [27] [Online]. Available: http://www.arcoptix.com/Q_Plate.htm?gclid=CLCZzeysjM4CFdiKaAodqqMLQA
- [28] M. Stalder and M. Schadt, "Linearly polarized light with axial symmetry generated by liquid-crystal polarization converters," *Opt. Lett.*, vol. 21, no. 23, pp. 1948–1950, 1996.
- [29] X. Liu and F. Buchali, "Intra-symbol frequency-domain averaging based channel estimation for coherent optical OFDM," *Opt. Exp.*, vol. 16, no., pp. 21944–21957, 2008.
- [30] F. Li, X. Li, J. Zhang, and J. Yu, "Transmission of 100-Gb/s VSB DFT-spread DMT signal in short-reach optical communication systems," *IEEE Photon. J.*, vol. 7, no. 5, Oct. 2015, Art. ID 7904307.